Science of the Total Environment 755 (2021) 142904

Contents lists available at ScienceDirect

Science of the Total Environment

journal homepage: www.elsevier.com/locate/scitotenv

Application of quantitative transcriptomics in evaluating the *ex vivo* effects of per- and polyfluoroalkyl substances on Atlantic cod (*Gadus morhua*) ovarian physiology

Essa Ahsan Khan [a], Xiaokang Zhang [b], Eileen Marie Hanna [b,1], Fekadu Yadetie [c], Inge Jonassen [b], Anders Goksøyr [c], Augustine Arukwe [a,*]

[a] Department of Biology, NTNU, Norway
[b] Computational Biology Unit, Department of Informatics, University of Bergen, Norway
[c] Department of Biological Sciences, University of Bergen, Norway

HIGHLIGHTS

- Combined *ex vivo* and transcript sequencing approach for fish ovarian toxicology
- Alteration of ovarian physiology by PFASs, given singly or as mixture
- PFASs altered functional enrichment of pathways belonging to integral biological processes.
- Highest PFOS and mixture exposures altered reproduction associated gene ontology terms.
- PFOS is the active component in mixture exposure scenario in altering normal ovarian functions.

GRAPHICAL ABSTRACT

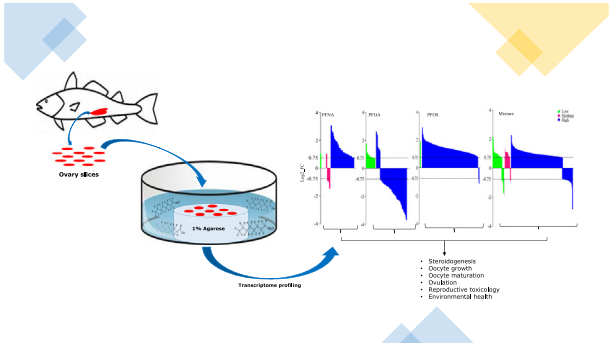

ARTICLE INFO

Article history:
Received 23 July 2020
Received in revised form 8 September 2020
Accepted 2 October 2020
Available online 14 October 2020

Editor: Daniel Wunderlin

Keywords:
PFASs
Ex vivo
Contaminants
Reproduction
RNA-seq
Environmental health

ABSTRACT

Because of their global consumption and persistence, per- and polyfluoroalkyl substances (PFASs), are ubiquitously distributed in the environment, as well as in wildlife and humans. In the present study, we have employed an *ex vivo* organ culture technique, based on the floating agarose method, of Atlantic cod ovarian tissue to investigate the effects of three different concentrations of PFOS, PFOA (1, 5 and 25 μM) and PFNA (0.5, 5 and 50 μM), used singly and in also in combination (1×, 20× and 100×). In the 1× exposure mixture, concentrations were decided based on their proportional levels (in molar equivalents) relative to PFOS, which is the most abundant PFAS in cod liver from a 2013 screening project. To investigate the detailed underlying mechanisms and biological processes, transcriptome sequencing was performed on exposed ovarian tissue. The number of differentially expressed genes (DEGs) having at least 0.75 $\log_2$-fold change was elevated in high, compared to low and medium concentration exposures. The highest PFNA, PFOA and PFOS concentrations, and the highest (100×) mixture exposure, showed 40, 68, 1295, and 802 DEGs, respectively. The latter two exposure groups shared a maximum of 438 DEGs. In addition, they both shared the majority of functionally enriched pathways belonging to biological processes such as cellular signaling, cell adhesion, lipid metabolism, immunological responses, cancer, reproduction and metabolism. Shortlisted DEGs that were specifically annotated to reproduction associated gene ontology (GO) terms were observed only in the highest PFOS and mixture exposure groups. These transcripts contributed to ovarian key events such as steroidogenesis (*star*, *cyp19a1a*), oocyte growth (*amh*), maturation (*igfbp5b*, *tgfβ2*,

* Corresponding author.
E-mail address: augustine.arukwe@ntnu.no (A. Arukwe).
[1] Current affiliation: Department of Computer Science and Mathematics, Lebanese American University, Byblos, Lebanon.

https://doi.org/10.1016/j.scitotenv.2020.142904

tgfβ3), and ovulation (*pgr*, *mmp2*). Contrary to other PFAS congeners, the highest PFOS concentration showed almost similar transcript expression patterns compared to the highest mixture exposure group. This indicates that PFOS is the active component of the mixture that significantly altered the normal functioning of female gonads, and possibly leading to serious reproductive consequences in teleosts.

1. Introduction

Per- and polyfluoroalkyl substances (PFASs) are anthropogenic contaminants of environmental, biota and human health concerns (Conder et al., 2008). Structurally, PFASs are composed of fully fluorinated hydrophobic alkyl chains with either alcohol, carboxyl, or a sulfonate terminal group (Conder et al., 2008). These unique chemical and structural properties render PFASs non-degradable (thermal stability and oxidation resistance) and persistent in the environment (Houde et al., 2006). The persistent nature of PFASs is fuelled by their use in different domestic and industrial applications such as surface treatment, surfactants, fire retardants, and coating materials (Co-operation, O. f. E, 2002). From 1950 until 2000, long-chain PFASs (greater than 8 carbons) were produced at an exponential rate (Lehmler, 2005). Later, they were voluntarily phased-out and substituted with shorter chain compounds (Lehmler, 2005). However, there has been a shift of PFASs production from Japan, Western Europe and the United States of America (USA) to China and India, making continental Asia the global hotspot for PFAS environmental contamination (Wang et al., 2014a; Wang et al., 2014b). Among the long-chain group, three most commonly used PFASs that are present at elevated levels in the environment include perfluorooctane sulfonate (PFOS), perfluorooctanoic acid (PFOA) and perfluorononanonanoic acid (PFNA) (Jantzen et al., 2016). Estimates showed that PFOS and PFOA were produced at 3500 and 500 metric tons, respectively, at the time when the phase-out began (Lau et al., 2007). Due to the broad commercial application of these compounds, many of the PFASs have been detected around the world in different geographical distributions from terrestrial to aquatic environments (Giesy and Kannan, 2001). They are present in the range of parts per trillion in the Atlantic, central Pacific and eastern Pacific ocean surface water (Yamashita et al., 2005; Zhang et al., 2019).

PFASs have a propensity to bioaccumulate in aquatic animals, where the bioaccumulation rate is directly proportional to PFASs carbon chain length (Houde et al., 2011). Additionally, PFASs functional groups also contribute to their accumulation in tissues. For example, the sulfonate end group is reported to bioaccumulate more, than those of the same carbon chain length with a carboxylate end group (Conder et al., 2008). Earlier statistics also showed the prevalence of PFOS in animal tissues to a greater extent. In North America, PFOS was found in the tissue of Polar bear (180–680 ng/g wet weight, ww), River otters (34–990 ng/g ww), Albatrosses (<35 ng/g ww), Bald eagles (1–2570 ng/g ww) and fish (21–87 ng/g ww). On the contrary, very few animal samples showed PFOA concentration above the detection limit (Giesy and Kannan, 2001). Likewise, in Norway's mainland and marine environments, PFOS have been reported at the highest levels in Harbour seal liver (66.3 ng/g ww), Herring gull egg (48.2 ng/g ww), Eider egg (10.1 ng/g ww) and Cod liver (0.59 ng/g ww), followed by perfluorinated carboxylic acids such as PFNA and perfluorotridecanoic acid (PFTrA) (Harju et al., 2013).

There is limited information on the long-term toxicity of PFASs to aquatic organisms (Directorate, OECD Environmental, 2002). Most of the studies that have been performed previously have focused primarily on early life stages of fish or amphibians and at high exposure concentrations. For example, reduced fathead minnow (*Pimephales promelas*) survival to PFOS exposure at a concentration of 1 mg/L was reported by Ankley and coworkers (Ankley et al., 2005). Likewise, Northern leopard frogs showed a delay in developmental rate to PFOS at a concentration of 10 mg/L (Ankley et al., 2004). There is still a significant knowledge gap in terms of toxicity of PFASs on other important life stages such as ovarian and testicular development and overt reproduction that has possible ecological consequences. It was hypothesized that PFASs could affect reproduction through alterations of the hypothalamic-pituitary-gonadal (HPG) axis (Preus Olsen et al., 2014). Earlier studies showed that rainbow trout and fathead minnows showed altered plasma concentration of androgen and estrogen after exposure to both PFOS and PFOA (Oakes et al., 2002; Oakes et al., 2004). Reduced testosterone (T) levels after PFOA exposure paralleled Cyp19a1a (aromatase: an enzyme that converts T to 17β-estradiol: E2) increase (Biegel et al., 1995; Liu et al., 1996).

The present study derived inspiration from the latest (2013) Norwegian environment screening report (Harju et al., 2013), showing the detection of different PFASs in the liver of cod from Norway's marine and coastal environments. We selected three long-chain PFASs (PFOS, PFOA, and PFNA) from this list, to investigate their effects on cod ovaries using individual or mixture exposure scenarios. *Ex vivo* organ culture technique based on a floating agarose method was employed to expose cod ovarian slices to these PFASs. We aimed to investigate the molecular basis of PFASs effect on ovarian physiology through changes in transcriptome profile. In addition, we wanted to perform functional analysis of transcriptomic data to investigate biological pathways that were affected, in order to produce predictive information as a tool for environmental monitoring and screening of PFAS effects on biota. Our hypothesis is that *ex vivo* exposure of cod ovary to organic contaminants (such as PFASs) will produce compound and concentration-specific alterations of transcript patterns in biological pathways, with direct consequences for ovarian physiology and reproduction success.

2. Materials and methods

2.1. Animals

Juvenile Atlantic cod were obtained from Havbruksstasjonen in Tromsø AS (Tromsø, Norway) and maintained at the Industrial and Aquatic Laboratory in Bergen (ILAB, Bergen, Norway). Fish were kept in 500 L tanks supplied with seawater at a temperature of 8–10 °C, 34 ppt (parts per thousand) salinity, 12:12 h light/dark cycle and fed with a commercial marine diet (Amber Neptune, Skretting, Stavanger, Norway). Before euthanizing to collect ovarian tissue for exposure, fish were approximately 18 months old, with mean body weight of 261 g (standard deviation (SD) = 59 g). The experimental setup was approved by the Norwegian Food Safety Authorities and performed accordingly (FOTS # 11730/17/18948).

2.2. Chemicals

DMSO (CAS No: 67-68-5), PFOS (CAS No: 2795-39-3), PFNA (CAS No: 335-67-1) and PFOA (CAS No: 72629-94-8) were purchased from Sigma-Aldrich (St. Louis, MO, U.S.A). All other chemicals were of highest commercially available grade.

2.3. Experimental design

Three PFASs (PFOS, PFOA, and PFNA) were used in this study and were selected based on the 2013 Norwegian environment screening report (Herzke et al., 2013). Concentrations were decided based on the proportional presence of different PFAS congeners, quantified in cod

liver from Northern Norway (Table S1) (Herzke et al., 2013). PFOS is the most abundant in the liver, and was used as a reference in calculating the relative abundance of other PFASs. For making a 1× PFAS mixture, concentration of PFOS was chosen based on the study conducted earlier by Bratberg et al. (2013) and liver bioaccumulation data as reported by Herzke et al. (2013). The concentrations of other compounds were determined by considering their relative abundance as discussed above, whose values are presented in SI Table S1. In addition, a 20× and 100× mixtures were used for high concentration exposures. Previously, a similar PFAS mixture that included PFTrA was used for *in vivo* exposure of cod (Khan et al., 2019). In addition to the mixture, single exposures were performed on ovarian slices at three different concentration levels, namely - low, medium and high (Table 1). A control group was prepared for each chemical. Ovarian slices from the same fish were distributed equally to control and individual exposure groups in order to minimize inter-exposure variations. In total five fish were used for each PFAS congener or mixture exposure. Out of these five individuals, ovarian slices from three fish were used for transcriptome sequencing.

2.4. Culturing of ovarian slices and exposure

This method of exposing tissue slices was adopted from the floating method using elder pith for culturing eel testicular tissue *ex vivo* (Nader et al., 1999). Later, Kortner and Arukwe (2007) validated this procedure by replacing the elder pith with an agarose cylinder (1% agarose) and used for exposing cod ovarian slices to organic contaminants and for evaluating reproductive endocrine physiology of fish.

Briefly, ovaries from juvenile female cod were dissected after sedation and kept on ice-cold Leibowitz-15 medium (Life Technologies™ Gibco®, Paisley, UK) and sliced manually with a sharp blade to achieve a final thickness of approximately 1 mm. Ovarian slices were cultured in 6-well plates on a floating agarose substrate covered with a nitrocellulose membrane. Culture media used in the present study was Leibowitz-15 medium supplemented with 0.1 mM L-aspartic acid, 0.1 mM L-glutamic acid, 1.7 mM L-proline, 10 mM Hepes (pH 7.4), 0.5% BSA and 1% penicillin-streptomycin-amphotericin (10,000 U/mL potassium penicillin, 10,000 μg/mL streptomycin and 25 μg/mL amphotericin B; Sigma-Aldrich). Cod ovarian slices were incubated at 10 °C with shaking at 50 rpm. Initially, ovarian slices were preincubated for 2 h followed by growth medium replacement with another medium containing either dimethyl sulfoxide (DMSO (0.01%): carrier vehicle) or PFOS, PFOA, and PFNA at three different concentrations, given individually or in a mixture (Table 1). After 72 h culture, ovarian slices were sampled and stored at −80 °C for RNA extraction. Another batch of slices was run in parallel in the same experimental setup for viability assay (TUNEL). Ovarian slices were fixed with 4% paraformaldehyde at 4 °C, followed by paraffinization and preparation of histological slides.

Table 1
Concentration of PFASs (PFOS, PFOA, and PFNA) used in the different *ex vivo* exposure scenarios with Atlantic cod ovarian slices, singly or in combination (mixture).

	Compounds	Concentration μM (mg/L)		
		Low	Medium	High
Individual exposure	PFOS	1 (0.5)	5 (2.5)	25 (12.5)
	PFOA	1 (0.41)	5 (2.07)	25 (10.4)
	PFNA	0.5 (0.23)	5 (2.32)	50 (23.2)
	Compounds	Concentration μM (mg/L)		
		1×	20×	100×
Mixture exposure	PFOS	0.067 (0.02)	1.35 (0.5)	6.77 (2.5)
	PFOA	0.012 (0.004)	0.25 (0.07)	1.25 (0.38)
	PFNA	0.017 (0.006)	0.35 (0.11)	1.73 (0.6)

2.5. RNA extraction and sequencing

Direct-zol™ RNA extraction kit (Zymo research corporation, Irvine, CA, U.S.A.) was used for extracting total RNA from frozen ovarian tissues (n = 3–6 per group), followed by RNA quantification and integrity confirmation using NanoDrop ND-1000 spectrophotometer (NanoDrop Technologies, Wilmington, DE, USA) and formaldehyde agarose gel electrophoresis, respectively. Total RNA (400 ng) was used for purifying poly(A)$^+$ RNA followed by fragmentation and preparation of complementary DNA (cDNA) library using guidelines of TruSeq® Stranded mRNA preparation kit. The Illumina HiSeq 4000 (Illumina, Inc., San Diego, CA, USA) platform was used to sequence the cDNA library to generate 75 bp (base pair) paired-end reads of 50 million depth.

2.6. Differential expression analysis (DEA)

To analyze the differential expression of genes, we used the pipeline developed by Zhang and Jonassen (2019). In brief, the FastQC v0.11.5 tool (http://www.bioinformatics.babraham.ac.uk/project/fastqc) was used for quality control, followed by reads alignment against available Atlantic cod genome gadMor1 using HISAT2 v2.1.0 tool (Star et al., 2011; Kim et al., 2015). FeatureCounts (from Subread 1.6.4) was used to generate read counts (Liao et al., 2014). Here, we set a threshold count per million (cpm) of ≥1, in at least two samples per comparison (between control and exposure groups). Genes passing threshold values were selected for differential expression analysis. The number of genes shortlisted while comparing each exposure group to their respective control group is shown in SI Table S2.

The differential expression of genes between control and exposure groups was determined by edgeR v3.18.1 using paired test and Trimmed Mean of M values (TMM) normalization and applying Benjamini-Hochberg method on the p-values to control the false discovery rate (FDR) (Robinson et al., 2010). Based on FDR (<0.05) and threshold $\log_2$-fold change of 0.75, the gene list was further shortened for functional analysis. The RNA-seq data have been deposited at European Nucleotide Archive (ENA) with accession number PRJEB39440.

2.7. Functional annotation

To investigate the functional implications of differentially expressed genes (DEGs), Molecular Signature Database (MSigDB) v7.1 under Gene Set Enrichment Analysis (GSEA) v4.0 tool (www.broad.mit.edu/gsea) was used in the present study. MSigDB has a collection of Kyoto Encyclopedia of Genes and Genomes (KEGG) gene sets that specifically indicate pathways affected by exposures. DEGs were mapped to KEGG gene sets. Significance levels were determined using software with inbuilt hypergeometric distribution test to examine enrichment of DEGs against identified genes. The pathway with a corrected p-value <0.05 is considered as significant. On the other hand, a custom gene set belonging to the hypothalamic-pituitary-gonadal (HPG) axis and reproduction-related biological processes were sorted using GO enrichment analysis tool (http://geneontology.org/) powered by PANTHER. Before functional analysis, human (*Homo sapiens*) orthologs of Atlantic cod genes were collected using Ensembl (http://www.ensembl.org) BioMart tool.

2.8. Real-time (quantitative) polymerase chain reaction (qPCR)

Reverse transcriptase (quantitative) polymerase chain reaction (RT-qPCR) was performed to quantify changes in the expression of seven (7) transcripts. Complementary DNA (cDNA) synthesis was performed using the iScript cDNA synthesis kit (Bio-Rad, Hercules, CA, USA). Followed by preparation of qPCR reaction mix (20 μL) containing - 5 μL of 1:6 diluted cDNA, 0.5 μM each of the forward and reverse primers, 1× iTaq SYBR green supermix with ROX (Bio-Rad Laboratories,

Hercules, CA, U.S.A.) and amplified using Mx3000P real-time PCR machine (Stratagene, La Jolla, CA). Detailed procedure for the quantification of transcript expression is presented in SI Section 1. Primer pair sequences used for transcript amplification are shown in SI Table S3.

2.9. Ovarian tissue viability assay

Terminal deoxynucleotidyl transferase dUTP nick end labeling (TUNEL) assay was performed to investigate the viability of *in vitro* culture of ovarian slices using the guideline of *in situ* apoptosis detection kit with Alexa Fluor™ dyes (Invitrogen, Cat# C10617). Before assay, tissue was fixed with 4% paraformaldehyde, paraffinized and cut into 5 μm slices. Finally, images were taken at 10× magnification using a fluorescence microscope.

2.10. Statistical analysis

The transcript expression results from the qPCR analysis were statistically analyzed using IBM SPSS Statistics 25. The statistical difference between control and exposure groups was determined using a paired *t*-test with the significance level set at $p \leq 0.05$. The majority of genes were normally distributed, except *cyp1c2*, *cyp19a1a*, and *mapk1* from some exposures. Therefore, their expression data were transformed using the logarithm function. This was statistically inspected using the Shapiro-Wilk test. Correlation between RNA-seq and qPCR data were evaluated using the Pearson correlation after fulfilling its assumptions.

3. Results and discussion

3.1. Viability of ovarian slices

Post-exposure viability of ovarian slices was evaluated using the TUNEL assay. The DNase treated positive control slices showed many TUNEL-positive cells, compared to ovarian slices from the control and exposure groups without nuclease treatment (Fig. 1). Previously, the same *ex vivo* organ culture technique was used to investigate testicular development and responses to contaminant exposures in fish, where the positive control group showed many TUNEL-positive cells (Celino et al., 2009). In contrast, the negative control group did not contain any TUNEL-positive cells. Our observations follow the earlier findings, demonstrating the cellular viability of the ovarian slices during the exposure periods and validating the observed transcriptional changes as PFASs exposure derived effects.

3.2. Transcript profiling and qPCR validation

The *ex vivo* PFAS mixture exposures at 1×, 20×, and 100× concentrations, produced 55, 13, and 802 DEGs, respectively (Table 2). The significantly higher number of DEGs at 100× mixture exposure indicates the potential alteration of reproductive physiology at this exposure concentration. Limited studies have been conducted to investigate the toxicological effects of PFASs on fish reproduction. Earlier, Ankley et al. (2005) studied the toxicity of PFOS on the development and reproduction of fathead minnow (*Pimephales promelas*), showing that PFOS exposure at 1 mg/L concentration for 14 days produced lethal effects on adults, while 0.23 mg/L (50% of effect concentration, EC50) altered fecundity after 21 days exposure. Female zebrafish (*Danio rerio*) showed a reduction in gonadosomatic index (GSI) after PFOS exposure at 0.05 and 0.25 mg/L for 70 days (Du et al., 2009). Long term exposure to PFOS at a concentration of 0.25 mg/L altered sex ratio, with a significant dominance of females (Du et al., 2009), suggesting the estrogenic effect of PFOS. Further, F1 progeny of exposed females (0.25 mg/L) showed severe deformities at early developmental stages, leading to 100% larval mortality (Wang et al., 2011). In contrast, Wang et al. (2011) and Keiter et al. (2012) did not observe any effects on survival in the F1 generation of zebrafish exposed to PFOS. However, 100% mortality was reported in the F2 generation after exposure to PFOS at 0.3 mg/L (Keiter et al., 2012).

Ovoviviparous swordtail fish (*Xiphophorus helleri*) also showed reproductive toxicities such as elevated GSI at 0.5 mg/L and *vtg* mRNA at 2.5 mg/L after 4-weeks exposure to PFOS (Han and Fang, 2010). Overall, approximately 0.25 mg/L of PFOS has been reported as an effective dose

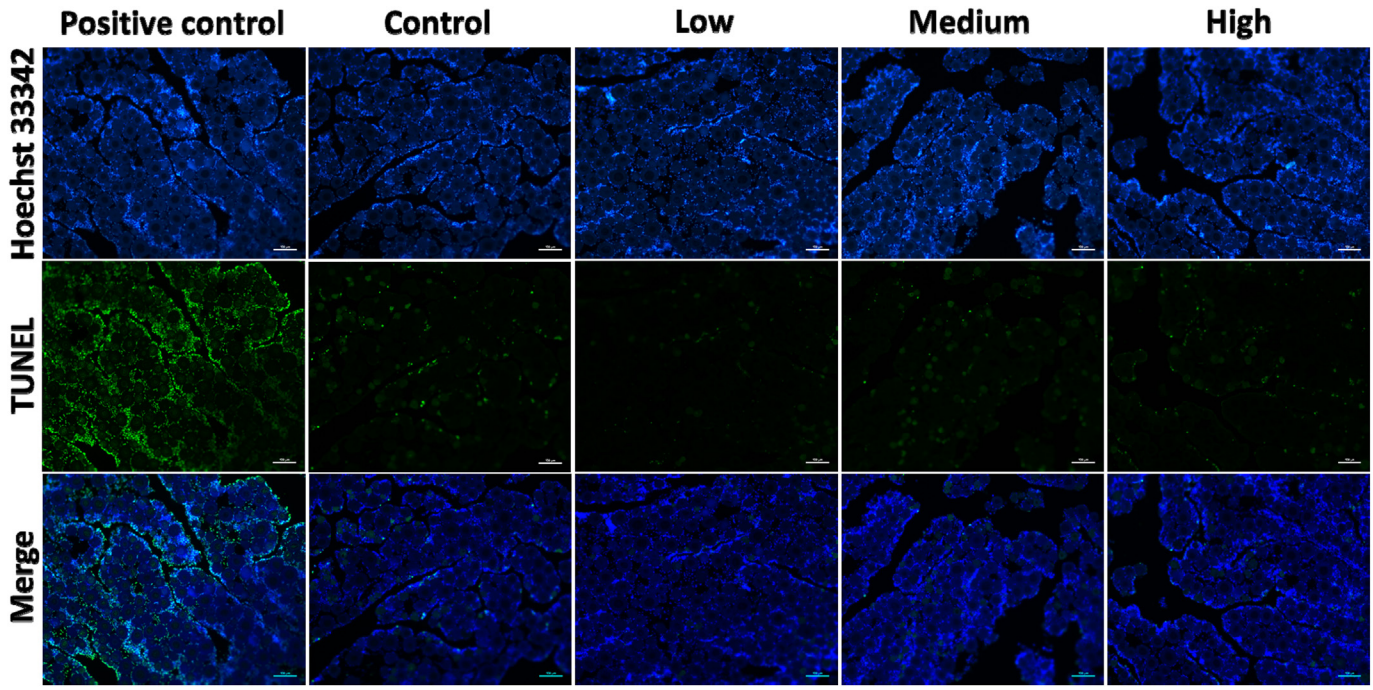

Fig. 1. Validation of Atlantic cod ovarian slice viability in the *ex vivo* floating agarose method using TUNEL assay. Positive apoptotic cells of ovarian tissues are shown in green fluorescence with fluorescent-modified nucleotide (*i.e.*, fluorescein-dUTP). The cell nucleus was stained with Hoechst 33342.

Table 2
Number and percentage (%) of DEGs in Atlantic cod ovarian slices exposed *ex vivo* to different concentrations of PFASs (PFOS, PFOA, and PFNA), singly or in combination (mixture).

	Compounds	Number (percent of DEGs)			Total DEGs
		Low	Medium	High	
Individual exposure	PFOS	1 (0.07%)	0	1295 (100%)	1295
	PFOA	15 (19.2%)	0	68 (87.2%)	78
	PFNA	1 (2.2%)	6 (13.3%)	40 (88.8%)	45
		Number (percent of DEGs)			Total DEGs
		1×	20×	100×	
Mixture exposure		55 (6.3%)	13 (1.5%)	802 (92.6%)	866

for the modulation of reproduction variable and was also maternally transferred to offspring at levels that produced embryo mortality (Han and Fang, 2010). In the present study, PFOS concentration in 20× exposure mixture exceeded the effective concentration level of 0.25 or 0.5 mg/L. Despite the presence of effective PFOS concentration in the 20× mixture, ovarian tissues did not show significant changes in the number of DEGs. Comparing Ankley et al. (2005) proposed concentrations to our designed mixtures, PFOS levels in the 100× exposure exceeded the lethality limit and might probably explain the observed large number of ovarian DEGs in the present study. However, there are no perfect guidelines from previous studies to relate toxicological responses across experimental models, as several studies have used different exposure conditions such as single or mixture exposure, concentration and exposure durations.

Besides PFOS, other PFASs including PFOA and PFNA were used in the exposure mixtures. Concerning available toxicological data, PFOA is ranked second in performing species sensitivity distribution (SSD) for the quantification of maximum acceptable concentration (MAC)-QS, indicating acute toxicity threshold, that for marine organisms is at 0.450 mg/L (Valsecchi et al., 2017). In contrast, the high exposure mixture (100×) represents a concentration that is below the acute toxicity threshold that may not necessarily play an active role in toxicological effects, compared to PFOS. Furthermore, limited PFNA toxicological data is available in marine organisms. Therefore, it is difficult to conclude on the involvement of PFOA and PFNA in the observed changes in transcript expression patterns. In order to understand the contribution of individual PFAS, single exposures at three different concentrations (low, medium and high), were also used for *ex vivo* exposure of ovarian tissue. To understand the possible mechanism of action of contaminants on biological processes, there is a need to perform experiments with relatively higher concentrations to elicit effects that can be extrapolated to lower or environmentally-relevant concentration (Lema et al., 2007). In the present study, the concentrations of PFASs used at high single exposures are more than double the amount used for 100× mixture exposure.

The individual high concentration exposures of PFOS, PFOA and PFNA produced a larger number of DEGs, compared to both low and medium concentrations, with respective 1295, 68 and 40 DEGs (Table 2). Based on transcript differential expression profile, PFOS produced profound effects on ovarian physiology, compared to PFOA and PFNA. Earlier studies have ranked PFOS as the most toxic PFAS, followed by PFOA and PFNA (Zheng et al., 2012; Ulhaq et al., 2013). The properties of PFOS such as the sulfonic group, renders the compound more hydrophobic and increases the bioaccumulation potential, compared to the carboxylic group containing compounds, such as PFOA and PFNA. Our findings are consistent with other toxicological patterns that were observed in previous studies evaluating the toxic effects of PFASs on zebrafish embryos (Zheng et al., 2012; Hagenaars et al., 2011). These findings were further strengthened by toxicity tests on Daphnia and other fish species (Giesy et al., 2010).

The observed changes in transcript expression patterns are different between single and mixture exposures. For example, at 100× PFAS mixture (containing 2.5 mg/L of PFOS), a total of 802 differentially expressed transcripts were observed. In contrast, no significant changes were observed when these concentrations were given singly, also for both PFOA and PFNA. Our findings are consistent with a previous report showing that the exposure of a primary culture of rare minnow (*Gobiocypris rarus*) hepatocytes to PFOS, singly, produced significant changes in a limited number of transcripts, compared to mixture exposures, which produced a higher number of transcripts (Wei et al., 2009). Thus, substantiating the different modes of action for single chemical and mixture exposure conditions. The most plausible interpretation for the observed differences in transcript expression patterns is that complex mixture exposure may alter physiological processes at various biological levels - including signal transduction, metabolism, regulation of transcription and post-translational modifications. In addition, individual PFASs may transiently regulate or alter the expression of a distinct set of transcripts whose effects may trigger other physiological cascades with overt reproductive consequences for fish. Thus, exposure to multiple PFASs may elicit novel signaling patterns that affect the global transcript regulation in organisms.

Representative transcripts from the RNA-seq data were selected for verification using RT-qPCR. The results are presented in the form of correlation-plot between the log2 fold-change values obtained from both RNA-seq and RT-qPCR (Fig. 2). The Pearson correlation coefficient, $r = 0.76$ ($p < 0.0001$), showed strong positive relationships between the two analytical approaches.

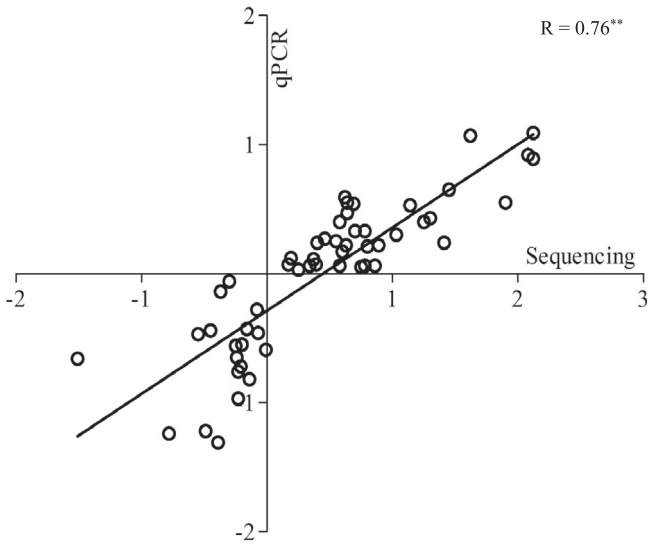

Fig. 2. Reverse-transcriptase quantitative polymerase chain reaction (RT-qPCR) validation of differentially expressed RNA sequencing (RNA-seq) genes, in cod ovarian slices ($n = 5$) exposed *ex vivo* to different concentrations of PFASs (PFOS, PFOA, and PFNA), given singly or in combination (mixture). The linear regression line represents a positive association at a significant Pearson correlation coefficient of $r = 0.76$ ($p < 0.0001$).

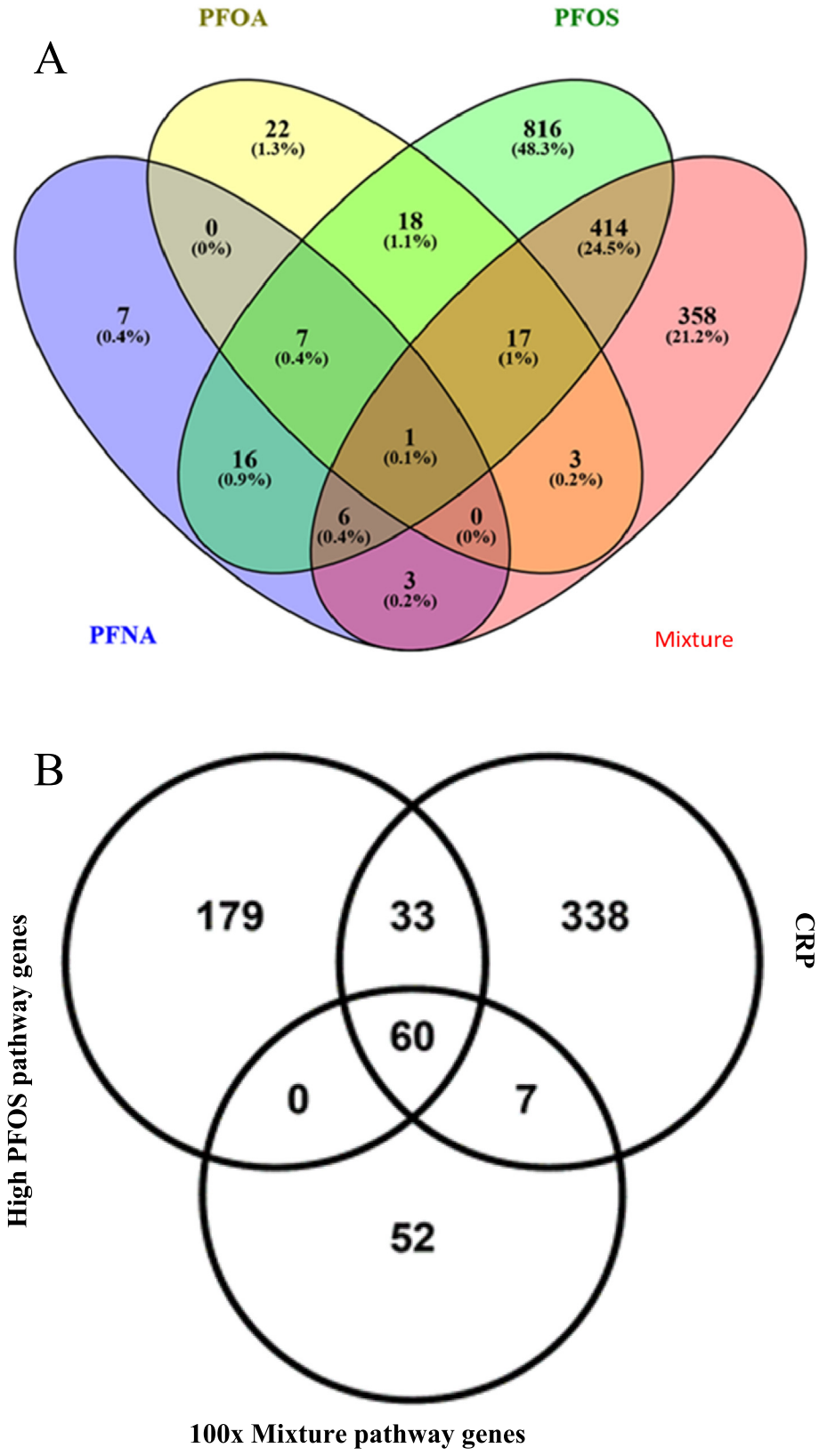

Fig. 3. Venn diagram of differentially expressed genes (DEGs) in high PFOS, PFOA, PFNA concentrations and 100× mixture exposures (A). Genes significantly responding to treatments of Atlantic cod ovarian slices after exposure to PFOS (25 μM), PFOA (25 μM), PFNA (50 μM), and 100× mixture (6.77 μM, 1.25 μM, and 1.73 μM, each of PFOS, PFOA and PFNA, respectively) were compared. DEGs from both the high PFOS and 100× mixture exposures were significantly enriched in KEGG pathways and compared to the genes that are common between the respective exposures, common response profile (CRP) (B). Actual number of DEGs in high PFOS and 100× mixture that are significantly enriched in KEGG pathways and CRP are presented in the Venn diagram.

3.3. Functional enrichment analysis

Functional enrichment analysis was conducted to understand the biological implications of DEGs on cellular pathways affected by different PFASs, given singly and as a mixture. Several affected pathways were identified in the high PFOS concentration and 100× mixture exposures. These numbers were proportional to the number of DEGs, with the highest significant pathways (87) that were enriched in high PFOS concentration, followed by a 100× mixture that contained 34 pathways (SI Table S4). Except for a few, the majority of pathways in the 100× mixture group are common with those affected in the high PFOS exposure. This indicates that PFOS contributed significantly to the effects observed in the mixture exposure (see also the profile of DEGs). The 100× mixture exposure shared 438, 21 and 10 DEGs with the high concentration of PFOS, PFOA and PFNA, respectively (Fig. 3A). The highest number of common DEGs (438) is denoted with a common response profile (CRP), sharing 34 and 56% in high PFOS concentration and 100× mixture pathway associated transcripts, respectively (Fig. 3B). The remaining transcripts (66%) in high PFOS concentration were unique, probably due to the differences between the concentration of PFOS used in the high and 100× mixture exposures. In addition, PFAS mixtures elicited transcript expression changes that were different from single exposure and as described previously by Wei et al. (2009), where PFOS exposure alone produced few DEGs, compared to when given in a mixture with other PFASs. It should be noted that, when given singly, the concentration of PFOS (2.5 mg/L) used in the 100× mixture did not elicit any changes in transcript pattern. Therefore, PFOS at 12.5 mg/L (which is 5× of the medium concentration) used for a high exposure concentration provided significant insight in understanding the contribution of PFOS in the mixture effects on transcript expression patterns.

The biological pathways that are common between high PFOS and 100× mixture belong to important processes categorized into general terms such as: cellular signaling, adhesion, cytoskeleton remodeling, lipid metabolism, ovarian development, and cancer (SI Table S5). Earlier, Khan et al. (2020) reported that these biological processes were also sensitive to contaminant exposure in cod ovary. Among cellular signaling, the transforming growth factor-β (Tgfβ) pathway was significantly affected. The *tgfb1*, *tgfb2* and *tgfb3* transcripts were up-regulated in the cod ovary, after the exposures (SI Table S6b and j). Previous studies have reported the importance of Tgfβ pathway on the development of ovarian follicle (Knight and Glister, 2006). There is limited information in the literature for discussing the modulations in the expression levels of *tgfb* transcripts, after exposure to either EDCs or PFASs, in particular. Other pathways such as Mapk- and Wnt-signaling, which are essential for sex determination and reproduction (Zhang et al., 2018; Du et al., 2017), were also affected in response to the high PFOS and 100× mixture exposures (SI Table S5). Exposure to PFOS alone elevated Mapk mediated oxidative stress pathways in zebrafish embryos (Shi and Zhou, 2010). Here, it was suggested that PFOS mediated transcript modulation was through Wnt/β-catenin signaling pathway (O'Brien et al., 2011).

Apoptotic and pro-apoptotic (p53 signaling) pathways that play integral roles in ovary-to-testis transformation were shown to be affected in juvenile zebrafish (Uchida et al., 2002; Rodriguez-Mari et al., 2010). Our data also showed the enrichment of both pathways in the cod ovary (SI Table S5), indicating the modulation of ovarian physiology. Exposure of white sucker (*Catostomus commersoni*) to bleached kraft pulp mill effluent altered reproductive endocrine homeostasis through high ovarian cell apoptosis (Janz et al., 2001). Endocrine-disrupting effects of contaminants on reproductive tissues could be assessed by examining their impact on chemokine signaling (Hall and Korach, 2013). In the present study, elevated expression levels of C-X-C motif chemokine ligand 14 (*cxcl14*) transcript was probably affected by chemokine signaling and in turn may alter reproductive outcomes.

We observed that a set of DEGs from significantly affected pathways are involved in cell adhesion and regulation of cytoskeleton homeostasis. Among others, the expression of collagen type V (*col5a2*), collagen type VI (*col6a1*), and integrin subunit beta 1 (*itgb1*) transcripts in cod ovary were up-regulated after the exposures (SI Table S6b and j). These transcripts contribute structurally and functionally to the components of extracellular matrix (ECM), whose modulation may lead to serious effects on the survival, proliferation, and steroidogenesis of granulosa cells, as reported previously by Le Bellego et al. (2005). In zebra pleco (*Hypancistrus zebra*) ovary, immunohistochemical analysis showed the accumulation of type IV collagen (collagen type V and VI paralogues) in theca cells of stage IV oocytes (Viana et al., 2018), whose expressions were shown to be regulated through androgen response elements (AREs) (Rolland et al., 2013). This suggests that EDCs may alter the ECM components through the androgen receptor (Ar). Herein, we observed that *ar* transcript was up-regulated after PFOS exposure, as well as changes in levels of ECM transcripts, suggesting that PFASs may interfere with Ar signaling in cod ovary. The cytoskeleton homeostasis predicted pathways is in accordance with previous findings showing that PFOS produced a disorganization of the actin-based cytoskeleton in primary culture of rodent and human Sertoli cells (Mao et al., 2018).

Lipid metabolism, including glycerophospholipid metabolic pathway, was significantly affected in both high PFOS and 100× mixture exposures. We observed that diacylglycerol kinase-alpha (*dgka*), -eta (*dgkh*), glycerol-3-phosphate acyltransferase 3 (*gpat3*), and phospholipid phosphatase 3 (*plpp3*) transcripts were up-regulated in cod ovary, after the exposures (SI Table S6b and j). Consistent with our data, Guan et al. (2018) had previously reported an association between glycerophospholipid metabolism and ovarian developmental stages. Our observation was further supported by a previous report showing that exposure to PFASs modulated lipid metabolites that are associated with glycerolipid and glycerophospholipid classes (Salihovic et al., 2018). Exposure to PFAS mixture was also shown to modulate lipid metabolism in cod liver (Dale et al., 2020).

Pathways belonging to immunological system such as cytokine-cytokine receptor interaction and leukocyte trans-endothelial migration were significantly affected in both high PFOS and 100× mixture exposures. High PFOS concentration affected additional immunological pathways such as B cell receptor signaling, natural killer cell-mediated cytotoxicity and others (SI Table S5). Such differences are probably due to the different PFOS concentration used in 100× mixture and high PFOS exposures. Previous studies have reported the immunomodulatory effects of legacy (PCBs) and emerging compounds, such as halogenated flame retardants (Waugh et al., 2018; Castaño-Ortiz et al., 2019). Compromised immune system enhances the susceptibility of fish ovaries to infections (Vidal-Dorsch et al., 2012). Our data showed a set of DEGs that are in the significantly enriched pathways, belong to infection processes (SI Table S5). Combined gonad infection and immunological responses can negatively affect reproductive capability (Williams, 2009).

Progesterone mediated oocyte maturation is the only pathway that was specifically enriched in ovarian physiological modulations in both high PFOS and 100× mixture exposure. These exposures produced significant elevation of progesterone receptor (*pgr*) transcript in cod ovary (SI Table S6b and j). Elevated expression of *pgr* in the ovary has been shown to induce early oocyte maturation through *pgr*-mediated signaling pathways (Aizen et al., 2018). Although there are limited data on the modulation of *pgr* after exposure to PFASs, other EDCs such as diethanolamine and tetrachloroethylene have been reported to respectively repress and induce basal expression of estrogen-responsive *pgr* transcript (Alofe et al., 2019). In addition, other pathways associated with ovarian physiology such as the gonadotropin releasing hormone (GnRH) signaling, steroid hormone biosynthesis, and oocyte meiosis were affected only in the high PFOS group (SI Table S5).

Both PFOA and PFNA contributed to very few DEGs. As a result of these small number of DEGs, no significant enrichment of pathways was observed. Individually, these exposures did not produce functional

alterations. However, this does not, by any means, underestimate their potential contribution in the observed mixture effects. Some DEGs in the high PFOA and PFNA exposures were also observed in the 100× mixture exposure and are part of pathways affected in the mixture exposure. For example, bone morphogenetic protein 4 (*bmp4*) transcript was differentially expressed after exposure to high PFOA and 100× mixture and participated in tgfβ signaling and cancer pathways at the mixture exposure. Likewise, cAMP-responsive element binding protein 5 (*creb5*) transcript was differentially expressed at high PFNA and 100× mixture exposures and participated in cancer pathways in the mixture exposure. Contrary to the transcripts discussed earlier, some DEGs that are common between high PFOA/PFNA and 100× mixture, belong to CRP. This indicates that both PFOS and PFOA/PFNA contributed to the modulations in the expression of those transcripts in the mixture exposure group. For example, the inhibitor of nuclear factor-kappa B kinase subunit beta (*ikbkb*) belonging to the CRP, was differentially expressed at high PFNA and participated in the majority of pathways affected by the 100× mixture exposure. A key observation was that each biological process has a set of pathways that are comparatively larger in high PFOS, compared to 100× mixture exposure (SI Tables S4 and S5). The differences in effects can only be attributed to the concentration differences between the individual high PFOS exposure, that modulated the expression of a larger number of transcripts, which in turn affected more pathways.

3.4. Reproductive physiology profiling

To address biological consequences in the context of reproduction physiology, DEGs were annotated to GO terms associated with reproduction. Except for high PFOS and 100× mixture, the rest of the exposures have few DEGs and lack annotation to selected GO terms. Out of 1295 DEGs of high PFOS exposure, 128 were annotated to "reproduction" (GO:0000003). Other reproduction-related GO terms including "reproductive system development" (GO:0061458), "ovulation cycle" (GO:0042698), "female gamete generation" (GO:0007292), "regulation of steroid metabolic process" (GO:0019218) were identified and shared transcripts with the highly representative term, GO:0000003 (Table 3). On the other hand, 100× mixture has fewer DEGs (73) annotated to "reproduction" (GO:0000003). Other reproduction-related GO terms are presented in Table 3. Both high PFOS and 100× mixture shared 49 transcripts, as represented in the Venn diagram (Fig. 4). This indicates that PFOS dominated other mixture components for the modulation of reproductive related genes in the ovary. Previous laboratory studies on the impact of individual endocrine-active chemicals on these transcripts reported some of the same responses, as those observed in the present study (Vang et al., 2007; Moore et al., 2011; Takahashi et al., 2019; Munier et al., 2016).

Some of the overlapping transcripts regulate ovarian key events. For example, a transcript of steroidogenesis acute regulatory (*star*) protein was up-regulated in both high PFOS and 100× mixture exposures (Fig. 4). The Star protein plays an important role in the uptake and transfer of cholesterol across the mitochondrial membrane as the rate-limiting step in steroidogenesis (Miller, 2007). Exposure to the synthetic pharmaceutical endocrine disruptor, 17α-ethynylestradiol (EE2) resulted in a similar response, showing a concentration-dependent increase of the Star protein in follicular cells (Vang et al., 2007). During ovarian steroidogenesis, androgens are metabolized to estrogens by cytochrome P450 aromatase (Cyp19a1a) (Callard et al., 2001). Previously, Lee et al. (2013) demonstrated the correspondence between plasma E2 levels and the expression of *star* and *cyp19a1a* transcripts in granulosa and theca cells. Herein, we observed that *cyp19a1a* and *star* transcripts showed parallel expression patterns in both high PFOS and 100× mixture exposures (Fig. 4).

Other transcripts that are important for oocyte growth, maturation and ovulation were differentially regulated in both high PFOS and 100× mixture exposures. For examples, anti-müllerian hormone (Amh) plays important role in regulating early ovarian development and late oocyte growth (Munsterberg and Lovell-Badge, 1991; Wu et al., 2010). Juvenile sex changes were shown to be altered through modulations in the expression of *amh* gene (Wu et al., 2010). Zebrafish (*Danio rerio*) male gonadal tissues showed significantly higher expression levels of *amh* transcripts, compared to female ovary (Rodríguez-Marí et al., 2005). Herein, elevated *amh* expression suggests a possible genotypic development of intersex characteristics in juvenile female cod to high PFOS and PFASs mixture, that may be phenotypically manifested after continuous long-term exposure. Previously, Wei et al. (2007) reported intersex characteristics in male rare minnows (*Gobiocypris rarus*) after long-term (28 days) exposure to PFOA.

Previous molecular studies have shown that different growth factors, such as insulin-like growth factors (*igfs*), Igf-binding proteins (*igfbps*) and members of the transforming growth factor beta (*tgfβ*) superfamily exhibit marked expression patterns throughout the preovulatory

Table 3
Reproduction associated gene ontology (GO) terms that are significantly affected by high exposure concentration of PFOS and 100× mixture.

Gene ontology (GO) terms	High PFOS		100× mixture	
	Number of genes	FDR	Number of genes	FDR
Reproductive process **(GO:0022414)**	118	4.83E−09	73	0.0000317
Reproduction **(GO:0000003)**	118	7.22E−09	73	0.0000328
Developmental process involved in reproduction **(GO:0003006)**	76	5.66E−05	48	0.00406
Multi-organism reproductive process **(GO:0044703)**	71	2.05E−03	–	–
Multicellular organism reproduction **(GO:0032504)**	57	2.64E−02	–	–
Multicellular organismal reproductive process **(GO:0048609)**	55	3.97E−02	–	–
Sexual reproduction **(GO:0019953)**	55	4.04E−02	–	–
Reproductive structure development **(GO:0048608)**	54	2.95E−09	35	0.00000315
Reproductive system development **(GO:0061458)**	54	3.96E−09	35	0.00000385
Sex differentiation **(GO:0007548)**	37	3.34E−07	20	0.00338
Development of primary sexual characteristics **(GO:0045137)**	33	3.33E−07	16	0.0158
Gonad development **(GO:0008406)**	32	5.76E−07	16	0.0124
Female sex differentiation **(GO:0046660)**	22	1.05E−06	12	0.00298
Development of primary female sexual characteristics **(GO:0046545)**	20	2.27E−06	9	0.0373
Female gonad development **(GO:0008585)**	19	4.52E−06	9	0.0279
Female gamete generation **(GO:0007292)**	15	2.10E−02	–	–
Regulation of steroid metabolic process **(GO:0019218)**	14	2.08E−02	–	–
Ovulation cycle **(GO:0042698)**	13	7.85E−04	9	0.0061
Ovulation cycle process **(GO:0022602)**	11	4.00E−04	6	0.0414
Ovarian follicle development **(GO:0001541)**	11	1.14E−03	–	–
Female genitalia development **(GO:0030540)**	–	–	4	0.0453

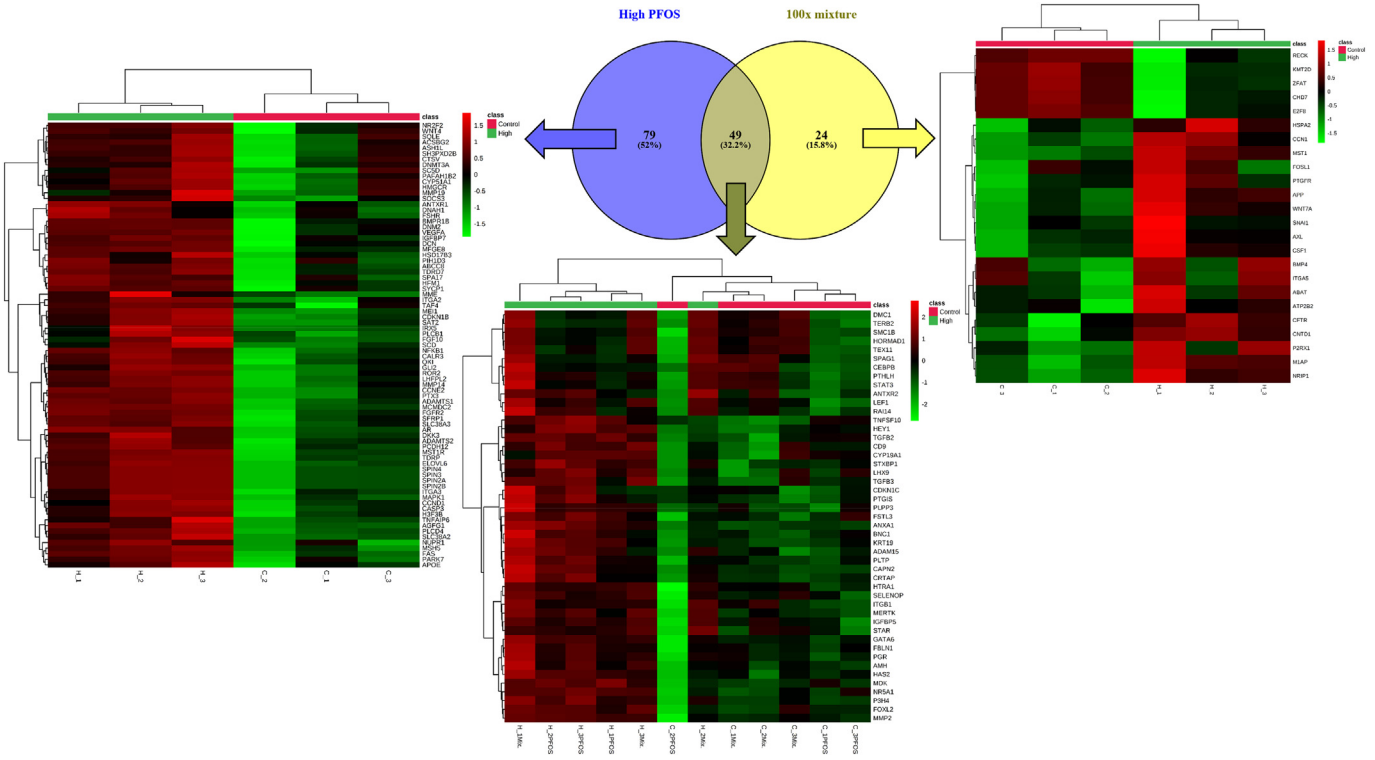

Fig. 4. A Venn diagram comparing differentially expressed genes (DEGs) belonging to reproductive physiology in high PFOS and 100× mixture exposures of Atlantic cod ovaries *ex vivo*. Normalized count (log-transformed) of genes in the individual sample is presented in the heat map. Rows represent genes and columns represent samples.

periods (Bobe et al., 2004; Kamangar et al., 2006). Exposure to high PFOS and 100× PFASs mixture produced significantly higher levels of *igfbp5b*, *tgfβ2* and *tgfβ3* transcripts in ovarian tissue (Fig. 4). In accordance with our findings, Moore et al. (2011) reported the alteration of Tgfβ superfamily signaling in gonadal tissue after exposure to environmental contaminants. In addition, ovulation associated progesterone receptor (*pgr*) and its regulatory protease, matrix metallopeptidase 2 (*mmp2*) (Ogiwara and Takahashi, 2017; Curry and Smith, 2006) were enriched in the cod ovary after high PFOS and 100× mixture exposures. Previously, granulosa synthesis of Pgr and its ligand were regulated by intracellular cyclic adenosine monophosphate (cAMP) levels and shown to be modulated by EDCs (Takahashi et al., 2019; Munier et al., 2016).

In our data, most of the reproduction related DEGs in 100× mixture overlapped with those of the high PFOS exposure. In contrast, a large proportion of DEGs were unique in the high PFOS group (Fig. 4). Although they are unique, they also participated in the same functions as shared DEGs. Some of the unique genes such as cytochrome P450 family 51 (*cyp51*), 3-hydroxy-3-methylglutaryl-CoA reductase (*hmgcr*), apolipoprotein E (*apoe*) and follicle-stimulating hormone receptor (*fshr*) are responsible for the biosynthesis and uptake of cholesterol, as well as steroidogenesis in teleost ovary (Leng et al., 2019; Skolness et al., 2013). It has been reported that HMG-CoA reductase activity was induced by estrogen receptor-α (Esr) agonists (Wang et al., 2006). The elevated expression of *hmgcr* in cod ovary suggests the estrogenic effects of PFOS. Previously, Rodríguez-Jorquera et al. (2018) reported the induction of vitellogenin (Vtg) by PFASs in a fathead minnow (*Pimephales promelas*) oligonucleotide microarray. The rationale for such unique responses may be attributed to the concentration and composition of the exposure mixture and PFOS exposure groups.

3.5. Environmental consequences of PFAS mixture

The current study was designed based on concentrations of different PFASs accumulated in cod tissue, caught from Norway's coastal and marine environment (Herzke et al., 2013). Countries that do not follow the phasing-out regime, may expect PFAS levels reaching a plateau where the 100× exposure mixture might be a relevant concentration for evaluating risk assessments. Only 1× exposure mixture has levels closest to what was measured in the mentioned screening project and could be used to evaluate health and reproduction risks fish species at Norway's mainland and coastal environments. However, environmental concentrations may exceed the 1× exposure mixture at PFASs contaminated areas. Contrary to 100×, a 1× exposure mixture effected the expression of very few transcripts (SI Table S4). In response to transcript changes, only the Mapk-signaling pathway was significantly enriched in the cod ovary. Previous studies have indicated the activation of Mapk-signaling pathway in the presence of reactive oxygen species (ROS). In the teleost hypothalamic-pituitary-gonadal (HPG) axis, gonadotropins ignite an inflammatory response in the follicles to generate ROS that may also activate the Mapk-signaling pathway and thereby play an indispensable role for ovulation (Shkolnik et al., 2011). Exposure to PFOS induced Mapk mediated oxidative stress pathways in zebrafish embryos (Shi and Zhou, 2010). Observation from the present study suggested that long-chain PFASs (PFOS, PFOA, and PFNA) in an environmentally realistic concentration mixture can affect ovarian physiology in cod.

CRediT authorship contribution statement

Essa Ahsan Khan: Conceptualization, Investigation, Formal analysis, Writing - original draft, Writing - review & editing. **Xiaokang Zhang:** Formal analysis, Writing - review & editing. **Eileen Marie Hanna:** Formal analysis, Writing - review & editing. **Fekadu Yadetie:** Conceptualization, Investigation, Formal analysis, Writing - review & editing. **Inge Jonassen:** Resources, Funding acquisition, Project administration, Writing - review & editing. **Anders Goksøyr:** Conceptualization, Resources, Funding acquisition, Project administration, Writing - review & editing. **Augustine Arukwe:** Conceptualization, Investigation, Formal analysis, Supervision, Resources, Funding acquisition, Project administration, Writing - original draft, Writing - review & editing.

Declaration of competing interest

The authors declare that there are no conflicts of interest associated with our study and paper

Acknowledgments

We thank the Research Council of Norway through the dCod 1.0: decoding systems toxicology of Atlantic cod project (Center for Digital Life Norway project no. 248840). The sequencing project at Genomics Core Facility (GCF) is supported in part by major grants from the Research Council of Norway (grant no. 245979/F50). We also acknowledge the Trond Mohn Foundation for the special prizes for RNA sequencing (grant no. BFS2016-genom).

Appendix A. Supplementary data

Supplementary data to this article can be found online at https://doi.org/10.1016/j.scitotenv.2020.142904.

References

Aizen, J., Pang, Y., Harris, C., Converse, A., Zhu, Y., Aguirre, M.A., Thomas, P., 2018. Roles of progesterone receptor membrane component 1 and membrane progestin receptor alpha in regulation of zebrafish oocyte maturation. Gen. Comp. Endocrinol. 263, 51–61.

Alofe, O., Kisanga, E., Inayat-Hussain, S.H., Fukumura, M., Garcia-Milian, R., Perera, L., Vasiliou, V., Whirledge, S., 2019. Determining the endocrine disruption potential of industrial chemicals using an integrative approach: public databases, in vitro exposure, and modeling receptor interactions. Environ. Int. 131, 104969.

Ankley, G.T., Kuehl, D.W., Kahl, M.D., Jensen, K.M., Butterworth, B.C., Nichols, J.W., 2004. Partial life-cycle toxicity and bioconcentration modeling of perfluorooctanesulfonate in the northern leopard frog (Rana pipiens). Environ. Toxicol. Chem. 23, 2745–2755.

Ankley, G.T., Kuehl, D.W., Kahl, M.D., Jensen, K.M., Linnum, A., Leino, R.L., Villeneuve, D.A., 2005. Reproductive and developmental toxicity and bioconcentration of perfluorooctanesulfonate in a partial life-cycle test with the fathead minnow (Pimephales promelas). Environ. Toxicol. Chem. 24, 2316–2324.

Biegel, L.B., Liu, R.C., Hurtt, M.E., Cook, J.C., 1995. Effects of ammonium perfluorooctanoate on Leydig-cell function: in vitro, in vivo, and ex vivo studies. Toxicol. Appl. Pharmacol. 134, 18–25.

Bobe, J., Nguyen, T., Jalabert, B., 2004. Targeted gene expression profiling in the rainbow trout (Oncorhynchus mykiss) ovary during maturational competence acquisition and oocyte maturation. Biol. Reprod. 71, 73–82.

Bratberg, M., Olsvik, P.A., Edvardsen, R.B., Brekken, H.K., Vadla, R., Meier, S., 2013. Effects of oil pollution and persistent organic pollutants (POPs) on glycerophospholipids in liver and brain of male Atlantic cod (Gadus morhua). Chemosphere 90, 2157–2171.

Callard, G.V., Tchoudakova, A.V., Kishida, M., Wood, E., 2001. Differential tissue distribution, developmental programming, estrogen regulation and promoter characteristics of cyp19 genes in teleost fish. J. Steroid Biochem. 79, 305–314.

Castaño-Ortiz, J.M., Jaspers, V.L., Waugh, C.A., 2019. PFOS mediates immunomodulation in an avian cell line that can be mitigated via a virus infection. BMC Vet. Res. 15, 214.

Celino, F.T., Yamaguchi, S., Miura, C., Miura, T., 2009. Arsenic inhibits in vitro spermatogenesis and induces germ cell apoptosis in Japanese eel (Anguilla japonica). Reproduction 138, 279–287.

Conder, J.M., Hoke, R.A., Wolf, W.d., Russell, M.H., Buck, R.C., 2008. Are PFCAs bioaccumulative? A critical review and comparison with regulatory criteria and persistent lipophilic compounds. Environ. Sci. Technol. 42, 995–1003.

Co-operation, O. f. E, 2002. Development, Co-operation on Existing Chemicals: Hazard Assessment of Perfluorooctane Sulfonate (PFOS) and Its Salts.

Curry, T.E., Smith, M.F., 2006. Impact of extracellular matrix remodeling on ovulation and the folliculo-luteal transition. Seminars in Reproductive Medicine. 2006. Copyright© 2006 by Thieme Medical Publishers, Inc, 333 Seventh Avenue, New, pp. 228–241.

Dale, K., Yadetie, F., Müller, M.B., Pampanin, D.M., Gilabert, A., Zhang, X., Tairova, Z., Haarr, A., Lille-Langøy, R., Lyche, J.L., 2020. Proteomics and lipidomics analyses reveal modulation of lipid metabolism by perfluoroalkyl substances in liver of Atlantic cod (Gadus morhua). Aquat. Toxicol. 105590.

Directorate, OECD Environmental, 2002. Hazard assessment of perfluorooctane sulfonate (PFOS) and its salts: ENV/JM/RD (2002) 17/final. Organisation for Economic Co-operation and Development.

Du, Y., Shi, X., Liu, C., Yu, K., Zhou, B., 2009. Chronic effects of water-borne PFOS exposure on growth, survival and hepatotoxicity in zebrafish: a partial life-cycle test. Chemosphere 74, 723–729.

Du, X., Wang, B., Liu, X., Liu, X., He, Y., Zhang, Q., Wang, X., 2017. Comparative transcriptome analysis of ovary and testis reveals potential sex-related genes and pathways in spotted knifejaw Oplegnathus punctatus. Gene 637, 203–210.

Giesy, J.P., Kannan, K., 2001. Global distribution of perfluorooctane sulfonate in wildlife. Environ. Sci. Technol. 35, 1339–1342.

Giesy, J.P., Naile, J.E., Khim, J.S., Jones, P.D., Newsted, J.L., 2010. Aquatic toxicology of perfluorinated chemicals. In Reviews of Environmental Contamination and Toxicology. Springer, pp. 1–52.

Guan, N.-N., Zhou, Q., Lan, T., Zhou, L.-F., Zhao, B.-W., Wang, W.-M., Gao, Z.-X., 2018. Is the nutritional value of fish fillet related to fish maturation or fish age? Integrated analysis of transcriptomics and metabolomics in blunt snout bream (Megalobrama amblycephala). Cell. Physiol. Biochem. 49, 17–39.

Hagenaars, A., Vergauwen, L., De Coen, W., Knapen, D., 2011. Structure–activity relationship assessment of four perfluorinated chemicals using a prolonged zebrafish early life stage test. Chemosphere 82, 764–772.

Hall, J.M., Korach, K.S., 2013. Endocrine disrupting chemicals promote the growth of ovarian cancer cells via the ER-CXCL12-CXCR4 signaling axis. Mol. Carcinog. 52, 715–725.

Han, J., Fang, Z., 2010. Estrogenic effects, reproductive impairment and developmental toxicity in ovoviparous swordtail fish (Xiphophorus helleri) exposed to perfluorooctane sulfonate (PFOS). Aquat. Toxicol. 99, 281–290.

Harju, M., Herzke, D., Kaasa, H., 2013. Perfluorinated alkylated substances (PFAS), brominated flame retardants (BFR) and chlorinated paraffins (CP) in the Norwegian environment–screening. Rapport M40–2013. Statlig Program for Forurensningsovervåking, Norwegian Ministry of the Environment, Oslo, Norway.

Herzke, D., Kaasa, H., Gravem, F., Gregersen, H., Jensen, J., Horn, J., Harju, M., Borgen, A., Enge, E., Warner, N., 2013. Perfluorinated Alkylated Substances, Brominated Flame Retardants and Chlorinated Paraffins in the Norwegian Environment-Screening 2013. Norwegian Environment Agency. NILU–Norsk Institutt for Luftforskning. SWECO, Tromsø, Norway.

Houde, M., Bujas, T.A., Small, J., Wells, R.S., Fair, P.A., Bossart, G.D., Solomon, K.R., Muir, D.C., 2006. Biomagnification of perfluoroalkyl compounds in the bottlenose dolphin (Tursiops truncatus) food web. Environ. Sci. Technol. 40, 4138–4144.

Houde, M., De Silva, A.O., Muir, D.C., Letcher, R.J., 2011. Monitoring of perfluorinated compounds in aquatic biota: an updated review: PFCs in aquatic biota. Environ. Sci. Technol. 45, 7962–7973.

Jantzen, C.E., Annunziato, K.A., Bugel, S.M., Cooper, K.R., 2016. PFOS, PFNA, and PFOA sublethal exposure to embryonic zebrafish have different toxicity profiles in terms of morphometrics, behavior and gene expression. Aquat. Toxicol. 175, 160–170.

Janz, D.M., McMaster, M.E., Weber, L.P., Munkittrick, K.R., Kraak, G.V.D., 2001. Recovery of ovary size, follicle cell apoptosis, and HSP70 expression in fish exposed to bleached pulp mill effluent. Can. J. Fish. Aquat. Sci. 58, 620–625.

Kamangar, B.B., Gabillard, J.C., Bobe, J., 2006. Insulin-like growth factor-binding protein (IGFBP)-1, -2, -3, -4, -5, and -6 and IGFBP-related protein 1 during rainbow trout postvitellogenesis and oocyte maturation: molecular characterization, expression profiles, and hormonal regulation. Endocrinology 147, 2399–2410.

Keiter, S., Baumann, L., Färber, H., Holbech, H., Skutlarek, D., Engwall, M., Braunbeck, T., 2012. Long-term effects of a binary mixture of perfluorooctane sulfonate (PFOS) and bisphenol A (BPA) in zebrafish (Danio rerio). Aquat. Toxicol. 118, 116–129.

Khan, E.A., Bertotto, L.B., Dale, K., Lille-Langøy, R., Yadetie, F., Karlsen, O.A., Goksøyr, A., Schlenk, D., Arukwe, A., 2019. Modulation of neuro-dopamine homeostasis in juvenile female Atlantic cod (Gadus morhua) exposed to polycyclic aromatic hydrocarbons and perfluoroalkyl substances. Environ. Sci. Technol. 53, 7036–7044.

Khan, E.A., Zhang, X., Hanna, E.M., Bartosova, Z., Yadetie, F., Jonassen, I., Goksøyr, A., Arukwe, A., 2020. Quantitative transcriptomics, and lipidomics in evaluating ovarian developmental effects in Atlantic cod (Gadus morhua) caged at a capped marine waste disposal site. Environ. Res. 189, 109906.

Kim, D., Langmead, B., Salzberg, S.L., 2015. HISAT: a fast spliced aligner with low memory requirements. Nat. Methods 12, 357–360.

Knight, P.G., Glister, C., 2006. TGF-β superfamily members and ovarian follicle development. Reproduction 132, 191–206.

Kortner, T.M., Arukwe, A., 2007. The xenoestrogen, 4-nonylphenol, impaired steroidogenesis in previtellogenic oocyte culture of Atlantic cod (Gadus morhua) by targeting the StAR protein and P450scc expressions. Gen. Comp. Endocrinol. 150, 419–429.

Lau, C., Anitole, K., Hodes, C., Lai, D., Pfahles-Hutchens, A., Seed, J., 2007. Perfluoroalkyl acids: a review of monitoring and toxicological findings. Toxicol. Sci. 99, 366–394.

Le Bellego, F., Fabre, S., Pisselet, C., Monniaux, D., 2005. Cytoskeleton reorganization mediates alpha6beta1 integrin-associated actions of laminin on proliferation and survival, but not on steroidogenesis of ovine granulosa cells. Reprod. Biol. Endocrin. 3, 19.

Lee, S.G., Kim, J.Y., Chung, J.-Y., Kim, Y.-J., Park, J.-E., Oh, S., Yoon, Y.-D., Yoo, K.S., Yoo, Y.H., Kim, J.-M., 2013. Bisphenol A exposure during adulthood causes augmentation of follicular atresia and luteal regression by decreasing 17β-estradiol synthesis via down-regulation of aromatase in rat ovary. Environ. Health Perspect. 121, 663–669.

Lehmler, H.-J., 2005. Synthesis of environmentally relevant fluorinated surfactants—a review. Chemosphere 58, 1471–1496.

Lema, S.C., Schultz, I.R., Scholz, N.L., Incardona, J.P., Swanson, P., 2007. Neural defects and cardiac arrhythmia in fish larvae following embryonic exposure to 2, 2′, 4, 4′-tetrabromodiphenyl ether (PBDE 47). Aquat. Toxicol. 82, 296–307.

Leng, X., Zhou, H., Tan, Q., Du, H., Wu, J., Liang, X., He, S., Wei, Q., 2019. Integrated metabolomic and transcriptomic analyses suggest that high dietary lipid levels facilitate ovary development through the enhanced arachidonic acid metabolism, cholesterol biosynthesis and steroid hormone synthesis in Chinese sturgeon (Acipenser sinensis). Br. J. Nutr. 122, 1230–1241.

Liao, Y., Smyth, G.K., Shi, W., 2014. featureCounts: an efficient general purpose program for assigning sequence reads to genomic features. J. Bioinform. 30, 923–930.

Liu, R.C., Hurtt, M.E., Cook, J.C., Biegel, L.B., 1996. Effect of the peroxisome proliferator, ammonium perfluorooctanoate (C8), on hepatic aromatase activity in adult male CrI: CD BR (CD) rats. Toxicol. Sci. 30, 220–228.

Mao, B., Mruk, D., Lian, Q., Ge, R., Li, C., Silvestrini, B., Cheng, C.Y., 2018. Mechanistic insights into PFOS-mediated Sertoli cell injury. Trends Mol. Med. 24, 781–793.

Miller, W.L., 2007. Steroidogenic acute regulatory protein (StAR), a novel mitochondrial cholesterol transporter. BBA-Mol. Cell. Biol. L. 1771, 663–676.

Moore, B. C.; Milnes, M. R.; Kohno, S.; Katsu, Y.; Iguchi, T.; Woodruff, T. K.; Guillette, L. J., Jr., Altered gonadal expression of TGF-beta superfamily signaling factors in

environmental contaminant-exposed juvenile alligators. J. Steroid Biochem. Mol. Biol. 2011, 127, 58–63.
Munier, M., Grouleff, J., Gourdin, L., Fauchard, M., Chantreau, V., Henrion, D., Coutant, R., Schiøtt, B., Chabbert, M., Rodien, P., 2016. In vitro effects of the endocrine disruptor p,p′-DDT on human follitropin receptor. Environ. Health Perspect. 124, 991–999.
Munsterberg, A., Lovell-Badge, R., 1991. Expression of the mouse anti-mullerian hormone gene suggests a role in both male and female sexual differentiation. Development. 113, 613–624.
Nader, M.R., Miura, T., Ando, N., Miura, C., Yamauchi, K., 1999. Recombinant human insulin-like growth factor I stimulates all stages of 11-ketotestosterone-induced spermatogenesis in the Japanese eel, Anguilla japonica, in vitro. Biol. Reprod. 61, 944–947.
Oakes, K., Martin, J., Sibley, P., Richards, S., Solomon, K., McLean, D., Van Der Kraak, G., 2002. In Evaluation of the Potential of Waterborne Perfluorooctanesulfonate and Perfluorooctanoic Acid in Promoting Endocrine Disruption and Oxidative Stress in Fish. 2002 pp. 16–20.
Oakes, K.D., Sibley, P.K., Solomon, K.R., Mabury, S.A., Van Der Kraak, G.J., 2004. Impact of perfluorooctanoic acid on fathead minnow (Pimephales promelas) fatty acyl-CoA oxidase activity, circulating steroids, and reproduction in outdoor microcosms. Environ. Toxicol. Chem. 23, 1912–1919.
O'Brien, J.M., Austin, A.J., Williams, A., Yauk, C.L., Crump, D., Kennedy, S.W., 2011. Technical-grade perfluorooctane sulfonate alters the expression of more transcripts in cultured chicken embryonic hepatocytes than linear perfluorooctane sulfonate. Environ. Toxicol. Chem. 30, 2846–2859.
Ogiwara, K., Takahashi, T., 2017. Involvement of the nuclear progestin receptor in LH-induced expression of membrane type 2-matrix metalloproteinase required for follicle rupture during ovulation in the medaka, Oryzias latipes. Mol. Cell. Endocrinol. 450, 54–63.
Preus Olsen, G., Olufsen, M.O., Pedersen, S.A., Letcher, R.J., Arukwe, A., 2014. Effects of elevated dissolved carbon dioxide and perfluorooctane sulfonic acid, given singly and in combination, on steroidogenic and biotransformation pathways of Atlantic cod. Aquat. Toxicol. 155, 222–235.
Robinson, M.D., McCarthy, D.J., Smyth, G.K., 2010. edgeR: a bioconductor package for differential expression analysis of digital gene expression data. J. Bioinform. 26, 139–140.
Rodríguez-Jorquera, I.A., Colli-Dula, R.C., Kroll, K., Jayasinghe, B.S., Parachu Marco, M.V., Silva-Sanchez, C., Toor, G.S., Denslow, N.D., 2018. Blood transcriptomics analysis of fish exposed to perfluoro alkyls substances: assessment of a non-lethal sampling technique for advancing aquatic toxicology research. Environ. Sci. Technol. 53, 1441–1452.
Rodríguez-Marí, A., Yan, Y.-L., BreMiller, R.A., Wilson, C., Canestro, C., Postlethwait, J.H., 2005. Characterization and expression pattern of zebrafish anti-Müllerian hormone (amh) relative to sox9a, sox9b, and cyp19a1a, during gonad development. Gene Expr. Patterns 5, 655–667.
Rodriguez-Mari, A., Canestro, C., BreMiller, R.A., Nguyen-Johnson, A., Asakawa, K., Kawakami, K., Postlethwait, J.H., 2010. Sex reversal in zebrafish fancl mutants is caused by Tp53-mediated germ cell apoptosis. PLoS Genet. 6, e1001034.
Rolland, A.D., Lardenois, A., Goupil, A.-S., Lareyre, J.-J., Houlgatte, R., Chalmel, F., Le Gac, F., 2013. Profiling of androgen response in rainbow trout pubertal testis: relevance to male gonad development and spermatogenesis. PLoS One 8, e53302.
Salihovic, S., Fall, T., Ganna, A., Broeckling, C.D., Prenni, J.E., Hyötyläinen, T., Kärrman, A., Lind, P.M., Ingelsson, E., Lind, L., 2018. Identification of metabolic profiles associated with human exposure to perfluoroalkyl substances. J. Exposure Sci. Environ. Epidemiol. 1.
Shi, X., Zhou, B., 2010. The role of Nrf2 and MAPK pathways in PFOS-induced oxidative stress in zebrafish embryos. Toxicol. Sci. 115, 391–400.
Shkolnik, K., Tadmor, A., Ben-Dor, S., Nevo, N., Galiani, D., Dekel, N., 2011. Reactive oxygen species are indispensable in ovulation. Proc. Natl. Acad. Sci. U. S. A. 108, 1462–1467.
Skolness, S.Y., Blanksma, C.A., Cavallin, J.E., Churchill, J.J., Durhan, E.J., Jensen, K.M., Johnson, R.D., Kahl, M.D., Makynen, E.A., Villeneuve, D.L., 2013. Propiconazole inhibits steroidogenesis and reproduction in the fathead minnow (Pimephales promelas). Toxicol. Sci. 132, 284–297.
Star, B., Nederbragt, A.J., Jentoft, S., Grimholt, U., Malmstrøm, M., Gregers, T.F., Rounge, T.B., Paulsen, J., Solbakken, M.H., Sharma, A., 2011. The genome sequence of Atlantic cod reveals a unique immune system. Nature 477, 207–210.
Takahashi, T., Hagiwara, A., Ogiwara, K., 2019. Follicle rupture during ovulation with an emphasis on recent progress in fish models. Reproduction 157, R1–R13.
Uchida, D., Yamashita, M., Kitano, T., Iguchi, T., 2002. Oocyte apoptosis during the transition from ovary-like tissue to testes during sex differentiation of juvenile zebrafish. J. Exp. Biol. 205, 711–718.
Ulhaq, M., Carlsson, G., Örn, S., Norrgren, L., 2013. Comparison of developmental toxicity of seven perfluoroalkyl acids to zebrafish embryos. Environ. Toxicol. Pharmacol. 36, 423–426.
Valsecchi, S., Conti, D., Crebelli, R., Polesello, S., Rusconi, M., Mazzoni, M., Preziosi, E., Carere, M., Lucentini, L., Ferretti, E., 2017. Deriving environmental quality standards for perfluorooctanoic acid (PFOA) and related short chain perfluorinated alkyl acids. J. Hazard. Mater. 323, 84–98.
Vang, S.-H., Kortner, T.M., Arukwe, A., 2007. Steroidogenic acute regulatory (StAR) protein and cholesterol side-chain cleavage (P450 scc) as molecular and cellular targets for 17α-ethynylestradiol in salmon previtellogenic oocytes. Chem. Res. Toxicol. 20, 1811–1819.
Viana, I.K.S., Gonçalves, L.A., Ferreira, M.A.P., Mendes, Y.A., Rocha, R.M., 2018. Oocyte growth, follicular complex formation and extracellular-matrix remodeling in ovarian maturation of the imperial zebra pleco fish Hypancistrus zebra. Sci. Rep. 8, 13760.
Vidal-Dorsch, D.E., Bay, S.M., Mays, M.A., Greenstein, D.J., Young, D., Wolf, J.C., Pham, D., Loguinov, A.V., Vulpe, C., 2012. Using gene expression to assess the status of fish from anthropogenically influenced estuarine wetlands. Environ. Sci. Technol. 46, 69–77.
Wang, H.H., Afdhal, N.H., Wang, D.Q., 2006. Overexpression of estrogen receptor α increases hepatic cholesterogenesis, leading to biliary hypersecretion in mice. J. Lipid Res. 47, 778–786.
Wang, M., Chen, J., Lin, K., Chen, Y., Hu, W., Tanguay, R.L., Huang, C., Dong, Q., 2011. Chronic zebrafish PFOS exposure alters sex ratio and maternal related effects in F1 offspring. Environ. Toxicol. Chem. 30, 2073–2080.
Wang, Z., Cousins, I.T., Scheringer, M., Buck, R.C., Hungerbühler, K., 2014a. Global emission inventories for C4–C14 perfluoroalkyl carboxylic acid (PFCA) homologues from 1951 to 2030, part I: production and emissions from quantifiable sources. Environ. Int. 70, 62–75.
Wang, Z., Cousins, I.T., Scheringer, M., Buck, R.C., Hungerbühler, K., 2014b. Global emission inventories for C4–C14 perfluoroalkyl carboxylic acid (PFCA) homologues from 1951 to 2030, part II: the remaining pieces of the puzzle. Environ. Int. 69, 166–176.
Waugh, C.A., Arukwe, A., Jaspers, V.L., 2018. Deregulation of microRNA-155 and its transcription factor NF-kB by polychlorinated biphenyls during viral infections. Apmis 126, 234–240.
Wei, Y., Dai, J., Liu, M., Wang, J., Xu, M., Zha, J., Wang, Z., 2007. Estrogen-like properties of perfluorooctanoic acid as revealed by expressing hepatic estrogen-responsive genes in rare minnows (Gobiocypris rarus). Environ. Toxicol. Chem. 26, 2440–2447.
Wei, Y., Shi, X., Zhang, H., Wang, J., Zhou, B., Dai, J., 2009. Combined effects of polyfluorinated and perfluorinated compounds on primary cultured hepatocytes from rare minnow (Gobiocypris rarus) using toxicogenomic analysis. Aquat. Toxicol. 95, 27–36.
Williams, B.A., 2009. Unique physiology of host–parasite interactions in microsporidia infections. Cell. Microbiol. 11, 1551–1560.
Wu, G.-C., Chiu, P.-C., Lyu, Y.-S., Chang, C.-F., 2010. The expression of amh and amhr2 is associated with the development of gonadal tissue and sex change in the protandrous black porgy. Acanthopagrus schlegeli. Biol. Reprod. 83, 443–453.
Yamashita, N., Kannan, K., Taniyasu, S., Horii, Y., Petrick, G., Gamo, T., 2005. A global survey of perfluorinated acids in oceans. Mar. Pollut. Bull. 51, 658–668.
Zhang, X., Jonassen, I., 2019. RASflow: An RNA-Seq Analysis Workflow With Snakemake. bioRxiv. p. 839191.
Zhang, Y., Miao, G., Fazhan, H., Waiho, K., Zheng, H., Li, S., Ikhwanuddin, M., Ma, H., 2018. Transcriptome-seq provides insights into sex-preference pattern of gene expression between testis and ovary of the crucifix crab (Charybdis feriatus). Physiol. Genomics 50 (5), 393–405.
Zhang, X., Lohmann, R., Sunderland, E.M., 2019. Poly-and perfluoroalkyl substances in seawater and plankton from the Northwestern Atlantic Margin. Environ. Sci. Technol. 53, 12348–12356.
Zheng, X.-M., Liu, H.-L., Shi, W., Wei, S., Giesy, J.P., Yu, H.-X., 2012. Effects of perfluorinated compounds on development of zebrafish embryos. Environ. Sci. Pollut. Res. 19, 2498–2505.